Anomalous Supercurrent Modulation in Josephson Junctions With Ni-Based Barriers

Burm Baek, Michael L. Schneider, Matthew R. Pufall, and William H. Rippard

***Abstract*—We investigate the supercurrent transport characteristics of Ni-barrier Josephson junctions with various barrier multilayer structures. Our device fabrication and magneto-electrical measurement methods provide high enough statistics and rigor necessary for the detailed characterization of magnetic Josephson junctions. As a result, we obtain the oscillatory critical current as a function of Ni thickness that matches the clean-limit transport theory except for certain anomalous features. Salient details include the finite oscillation phase shift due to a nonmagnetic spacer, the near-zero effective magnetic dead layer, and the distorted current-phase relationship near the 0-π transition. These allude to intricacies in the microscopic transport that are unique to certain magnetic Josephson junctions. We discuss a route toward a comprehensive understanding of realistic magnetic Josephson junctions based on the underlying effect of exchange field on the superconducting spin modulation.**

***Index Terms*—Josephson junctions (JJs), Josephson effect, magnetic devices, superconducting devices.**

I. Introduction

MAGNETIC device technologies have recently been under active investigation for application in superconducting electronics. Especially, the superconductor-ferromagnet (S-F) proximity effect has shown its potential to bring in the spintronic aspect for nonvolatile and scalable memory technologies: Studies on S-F hybrid structures have shown a way to manipulate the electronic spin state of the superconducting order [1]–[5], which would not be accessible in conventional superconducting electronics.

A prominent effect from such manipulation of the superconducting spin is the critical current oscillation as a function of the ferromagnetic barrier thickness in S-F-S Josephson junctions (JJs). The electron pairs coming from S to F occupy spin-dependent bands and the pair spin state can be converted between the conventional spin singlet and one of the triplet states. This conversion is roughly periodic with the F barrier thickness and results in the oscillatory Josephson coupling, including the reversal of the supercurrent (π phase) [1]–[3], [6], [7]. Such an oscillation has been measured for various ferromagnetic barriers [1], [4]. It has also been extended to spin-valve (SV) barriers to realize magnetically switchable JJs in the critical current or phase, which can be applied to superconducting memory [8]–[13].

So far, numerous experiments have shown the existence of such an oscillatory critical current in various materials. As the physical perspective and techniques improve and the need for technological application arises, more detailed and quantitative studies are being carried out around technologically important materials [13]–[18].

In this paper, we broadly present the features in the supercurrent transport in Ni-based JJs. Ni is a moderately strong, elemental ferromagnet, which presents a unique opportunity for investigating the regime of a clean-limit, ultrathin magnetic barrier in detail [19]–[22]. By use of proper methods, we minimize various uncertainties related to the control of the nanometer-scale thickness and magnetization and, consequently, we obtain clean critical current oscillation, which is also accompanied by subtle anomalous details.

II. Experiments

Our device fabrication and measurement methods are described in [15], which are summarized here. A typical device multilayer structure is Si/SiO_2/Nb(100)/Cu(5)/M/Cu(20)/Nb (100) (all thicknesses in nanometers), where M is the target barrier, which includes at least one Ni wedge layer. A wide range of Ni thickness is obtained on a single wafer by the wedge (nonuniform) film deposition, which removes a run-to-run variation and improves test device throughput substantially. Certain M includes $(Ni_{81}Fe_{19})_{69}Nb_{31}$ ("NiFeNb") spacers, which are not ferromagnetic at 4 K due to the heavy Nb-doping [15]. The multilayers are fabricated into micrometer-scale pillar devices in a circular or elliptical shape.

The devices are measured with the four-probe method in a liquid helium bath at 4 K. The magnetization of Ni is initially saturated by applying about 400 mT along the long axis. Subsequently, we remove trapped magnetic flux by heating and obtain the maximum supercurrent $I_m(H)$ and the normal resistance R_n by fitting the current–voltage characteristics to the resistively-shunted-junction model [see Fig. 1(a)] at a lower field range. $I_m(H)$ is typically a shifted Airy pattern as expected of circular or elliptical magnetic JJs [10]. Because the magnetic flux due

Manuscript received January 31, 2018; revised March 26, 2018; accepted April 26, 2018. Date of publication May 15, 2018; date of current version June 11, 2018. This work was supported in part by National Institute of Standards and Technology and in part by the IARPA Cryogenic Computing Complexity program. This paper was recommended by Editor-in-Chief B. Plourde. *(Corresponding author: Burm Baek.)*

The authors are with the National Institute of Standards and Technology, Boulder, CO 80305 USA (e-mail: burm.baek@nist.gov).

Color versions of one or more of the figures in this paper are available online at http://ieeexplore.ieee.org.

Digital Object Identifier 10.1109/TASC.2018.2836961

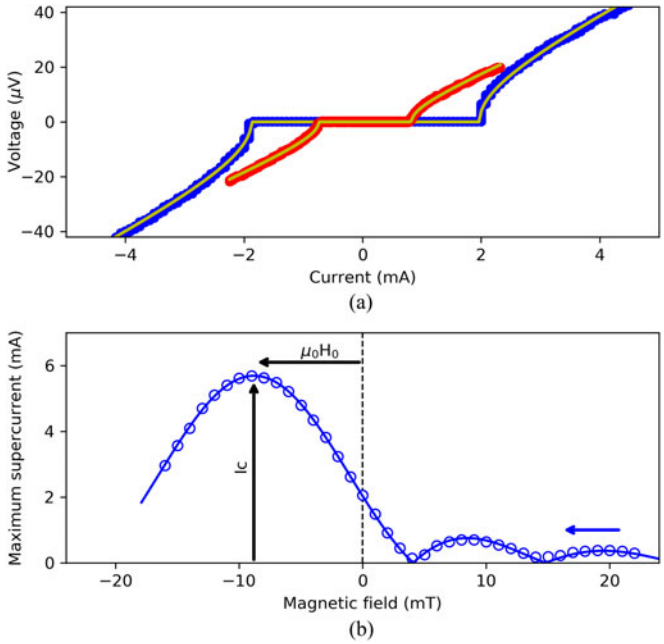

Fig. 1. Basic electrical characteristics of typical Nb/Cu/Ni/Cu/Nb JJs. (a) Typical current–voltage (*I–V*) characteristics. The wide-range (blue) and the narrow-range (red) *I–V* curves are measured from devices with 0.9- and 3.5-nm-thick Ni barriers, respectively. Yellow curves are fits. (b) Example of maximum supercurrent versus magnetic field. The magnetization of Ni is preset in the positive direction, resulting in the negative shift of the entire pattern. Symbols and curve are measured data and a fit for a downward sweep.

to the Ni magnetization can be canceled by an applied field in the opposite (negative) direction, the Airy pattern gives I_c (maximum I_m) at such a negative field offset H_0 [see Fig. 1(b)]. Most devices result in simple, field-offset Airy patterns without excessive distortion. This indicates a uniform and static (i.e., high switching field [10]) magnetization state of the barrier as well as minimal imperfection from the deposition and fabrication. Since the trivial remanent field effect is simply taken out at $H = H_0$ to extract the true I_c, these JJs are excellent approximations of idealized magnetic JJs for the study of the exchange field effect.

III. Results and Discussion

A. Field Offset Versus Thickness

Fig. 2 shows the field offset $H_0(d)$ with the Ni thickness d from barriers with different kinds of nonmagnetic spacers introduced in [15]. The apparent absence of data for Ni-barriers is due to too high I_c to measure from our device structure [13]. The simple linear trends come from the increased magnetic flux in the JJ proportional to the Ni thickness; the total magnetic flux $\Phi_{tot} \propto \mu_0 H_{rem}(d - d_{dead}) + \mu_0 H_0(2\lambda + d_{spacer} + d) = 0$ at $H = H_0$ and, thus, $H_0 \approx a(d - d_{dead})$ with $a \equiv -[H_{rem}/(2\lambda + d_{spacer})]$. Here, d_{dead} is the total magnetic dead layer thickness of Ni, λ is the penetration depth of the superconducting electrodes, and d_{spacer} is the total spacer thickness; $\mu_0 H_{rem}$ is the remanent field in Ni, which is about 0.5 T from the superconducting quantum interference device (SQUID) magnetometry on unpatterned Ni films. We note that the scatter is not completely random; rather, the data tend to get skewed in correlation with

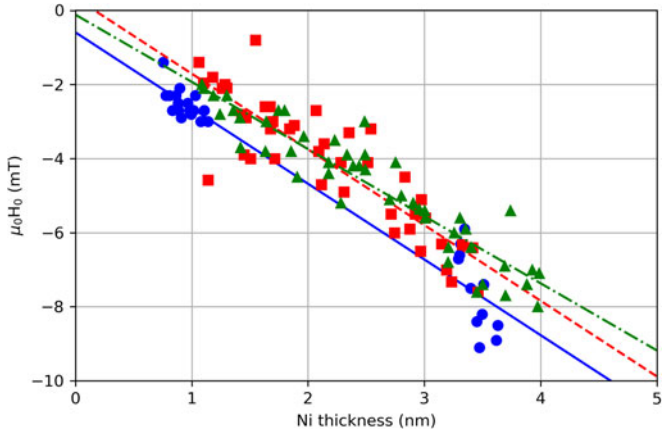

Fig. 2. Field offset of the Fraunhofer patterns versus Ni thickness for Ni (● and –), Ni/Cu(5)/NiFeNb(1.2) (■ and – –), and NiFeNb(1.2)/Cu(5)/Ni/Cu(5)/NiFeNb(1.2) (▲ and – ·) barriers. Symbols and lines are measured data and linear fits.

the dimensions, etc. Each fitted d_{dead} is smaller than the value obtained from SQUID magnetometry, 0.7 nm [15], but such a comparison is not statistically decisive due to the scatter in the data.

Nonideal effects may arises from either the superconducting or magnetic components. The above-mentioned model does not account for the long junction effect, which induces a nonuniform supercurrent distribution at the scale of the Josephson penetration depth for devices of a high critical current density (J_c) [23]. However, this discrepancy should be minimal for low-J_c devices that incorporate NiFeNb spacers. Nonuniform magnetization may cause statistical or geometry-dependent deviation in $I_m(H)$ and, thus, $H_0(d)$. For example, magnetic domains can be pinned to defects or the magnetization may curl in a small device due to finite exchange stiffness. A more comprehensive investigation may be necessary to understand the details and make this Josephson self-magnetometry an essential diagnostic tool for magnetic JJs.

B. Critical Current Versus Thickness

Fig. 3 shows the extracted oscillatory $V_c \equiv I_c R_n$, which can be treated as normalized I_c and is independent of the junction area. Unlike dirty-limit S-F-S devices with an exponentially fast decay, the $V_c(d)$ trend follows a clean-limit behavior with only moderate decay, as expected from an ultrathin, elemental ferromagnetic barrier. The measured $V_c(d)$ is fit by the numerical maximum of the clean-limit supercurrent $I_s(\varphi)$ derived in [24]

$$I_s = \frac{\pi\Delta\alpha^2}{2eR_n}\int_\alpha^\infty \frac{dy}{y^3}\left(\sin\frac{\varphi-y}{2}\tanh\frac{\Delta\cos\frac{\varphi-y}{2}}{2k_BT} + \sin\frac{\varphi+y}{2}\tanh\frac{\Delta\cos\frac{\varphi+y}{2}}{2k_BT}\right). \quad (1)$$

Here, φ is the superconducting phase difference across the JJ, Δ is the energy gap of the superconducting electrodes, and T is the temperature; $\alpha \equiv d/\xi$ with the characteristic oscillation length $\xi \equiv \hbar\nu_F/2E_{ex}$, the Fermi velocity ν_F, and the exchange energy E_{ex}.

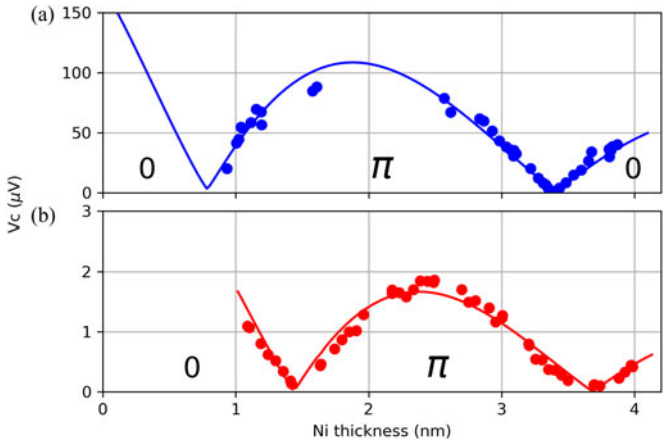

Fig. 3. V_c versus Ni thickness. (a) From Ni. (b) From NiFeNb(1.2)/Cu(5)/Ni/Cu(5)/NiFeNb(1.2) barriers. Symbols and curves are measured data and fits.

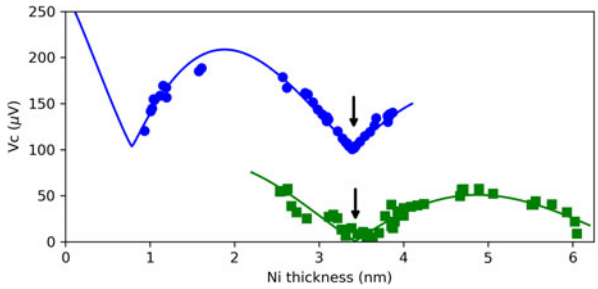

Fig. 4. V_c versus Ni thickness from Ni (●) and Ni/Cu(5)/Ni (■) barriers. Arrows mark the π-to-0 transition thicknesses obtained from the fit curves. Curves are fits. Ni data are offset by 100 μV for clarity.

C. Phase Shift Induced by a Spacer

As reported in [15] in detail, the inclusion of a NiFeNb layer is correlated with a shift in the $V_c(d)$ oscillation phase, while maintaining the overall trend of the clean-limit transport as characterized by the slow decay. Fig. 3 shows an example how substantial such a shift is. The fits shown in Fig. 3(a) and (b) result in -0.02 and 0.6 nm in the Ni thickness offsets, respectively. Such a phase shift also accompanies a slight change in the node-to-node period. These unexpected features suggest that the pair spin transport may be modified in a nontrivial way in a hybrid regime of a clean-limit ferromagnet and a dirty-limit spacer. A detailed theoretical insight might be given by extending the relevant quasiclassical theories [25] toward treating such a mixed transport regime.

D. Scatter in Critical Current Versus Thickness

The overall scatter and distortion are remarkably small, especially compared to $H_0(d)$. I_c is measured with an applied field that nullifies the total flux in the JJ. As mentioned for the nonideal $H_0(d)$ above, there may be finite nonuniform magnetization that cannot be canceled by an applied field. This induces slight nonuniform phase distribution, which reduces the local supercurrent from the peak value. Fortunately, such reduction in the local supercurrent is minimal if the magnetization nonuniformity is confined to small areas so the remaining local magnetic flux is small enough compared with the flux quantum. Furthermore, the impact is only of second order because this deviation is in reference to the peak value of the local maximum supercurrent. In contrast, the impact to the Josephson self-magnetometry is of first order (due to the linear trend at every point) and should be relatively more substantial, which is consistent with the larger scatter in Fig. 2.

E. Near-Zero Thickness Offset in Ni Devices

$V_c(d)$ of Ni devices are fit to the theory with a near-zero thickness offset -0.02 nm. This agrees with the near-zero offsets in $H_0(d)$ trends whereas it is quite different from the separate dead layer estimation of 0.7 nm derived from SQUID magnetometry (see Section III.A). Although a certain amount of discrepancy between different depositions is not uncommon, such a near-zero dead layer thickness is also in strong contrast to other studies of S-F hybrid structures (e.g., [21]).

However, another set of devices also supports the near-zero offset. We fabricated and measured devices with a barrier structure of Ni/Cu/Ni, where both Ni layers are nominally identical wedges with the same deposition duration. Effectively, this structure includes two additional Cu–Ni interfaces compared with single Ni devices. The offset due to the additional Cu–Ni interfaces should shift $V_c(d)$ by the added dead layer thicknesses. Here, we redefine d by the sum of the two Ni thicknesses. This method determines the offset induced at the interface in a purely experimental way without relying on a (less convincing) nonlinear fit to a theory. As a result, Fig. 4 clearly shows a negligible shift in the second phase-transition node.

These experimental results suggest a strong possibility of a near-zero offset in $V_c(d)$. Then, there arises the question whether this comes from a purely magnetic (i.e., the lack of a real magnetic dead layer) or other reasons. Even if there is a finite dead layer thickness, a small pair spin phase may be developed in the Cu side of the interfaces due to the inverse proximity effect. This may effectively move $V_c(d)$ negatively and reduce the positive offset expected from the dead layer. This effect may be prominent for a high-transparency interface; we find such theoretical cases of a small first-node thickness for transparent interfaces in [24]. Still, it would be quite coincidental if such an effect almost matched the dead layer offset.

F. 0-π Transition

The central feature of an S-F-S JJ is the transition of the ground state phase difference between 0 and π at the node thicknesses of the oscillatory $V_c(d)$. Fig. 5(a) shows the $V_c(d)$ of Ni devices near a node thickness 3.4 nm. We obtain devices with I_c suppressed by two orders of magnitude. Technologically, such a characteristic can be straightforwardly applied for SV JJ devices with nearly extinguishable I_c [10], [11]. Although a similar function can be implemented with, e.g., a conventional SQUID with an external magnetic flux control, SV JJs would not be limited by the requirement of a substantial SQUID loop size.

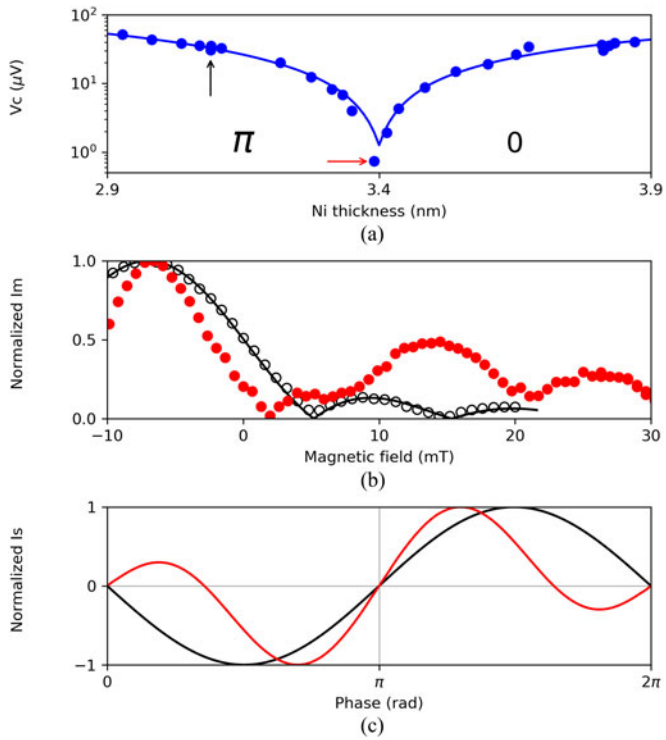

Fig. 5. Ni-barrier JJ properties near a 0-π transition thickness. (a) V_c versus Ni thickness. Symbols and curve are measurement data and a fit, respectively. (b) Normalized maximum supercurrent versus magnetic field. Red symbols are the measurement data from a near-node device with the lowest I_cR_n as marked by a red arrow in (a). Black symbols and curve are the measurement data and fit from a control device marked by a black arrow in (a). Both devices are of the same dimensions (1.5 μm $\times$ 3.0 μm ellipse). (c) Theoretical CPR. Solid red and black curves are from the near-node and control devices, as in the other panels.

Unfortunately, as the theoretical fit in Fig. 5(a) also suggests, I_c may not be completely extinguished at the 0-π transition node. Instead, we find an interesting, qualitative change in the supercurrent transport. Fig. 5(b) shows $I_m(H)$ of the devices near and away from the node as marked in Fig. 5(a). They are of the same lithographic dimensions for fair comparison. Clearly, $I_m(H)$ of the near-node device is distorted from a regular Airy pattern, unlike the other device. Since this regime is also of a low J_c, we rule out parasitic effects such as self-field and self-heating that may be present in high-J_c devices. We consistently find such distortion in near-node devices from different kinds of barrier structures and, thus, rule out a statistical anomaly. We note that such an irregular $I_m(H)$ also appears in [10, Fig. 3(c) and (d)] when the SV JJs are switched to a very low I_c state, i.e., a near-node state.

With such artifacts ruled out, the distorted $I_m(H)$ likely comes from a change in the underlying current-phase relationship (CPR) $I_s(\varphi)$ from the normal sinusoidal form $I_c\sin(\varphi)$ [27], [28]. In fact, Fig. 5(c), that uses the values calculated from (1), shows that $I_s(\varphi)$ should become nonsinusoidal near the node in theory, even without any extrinsic origin. Note that the first harmonics are inverted (i.e., shifted by π) because these are π-junctions with the Ni thicknesses between the first and the second nodes. The theoretical distortion near the transition is reasonably approximated by the appearance of the second harmonic component, which should result in corresponding, double-frequency features in $I_m(H)$. However, the experimentally obtained distortion in $I_m(H)$ in most devices is more irregular and varies widely between devices. This may imply the presence of an extrinsic cause as well. For example, even an atomic-level thickness nonuniformity in a device may have a substantial effect because of the extremely short length scale (about 1 nm) of the exchange field effect in Ni, which may result in the widely varying local CPR. Indeed, devices with artificially introduced thickness nonuniformity have been theoretically and experimentally studied to show that such a JJ can behave as if it has an effective CPR that is nontrivial in [29]–[31]. On the magnetic side, slight magnetic inhomogeneity may also induce nonuniformity in the local CPR that becomes appreciable only near the 0-π transition by locally changing the effective thickness or creating unintended equal-spin triplet supercurrents [32].

IV. Conclusion

We have characterized the supercurrent modulation due to the exchange field in Ni in detail. The oscillatory critical current due to Ni primarily validates the clean-limit theory but also reveals anomalous features worthy of further investigation, such as the deviation in the self-magnetometry, the phase shift due to a certain nonmagnetic spacer, the near-zero thickness offset in V_c(d) from the Cu–Ni interfaces, and the distorted CPR near a 0-π transition. Future research on these will provide a more complete insight into magnetic JJs and their technological implications for the future superconducting electronics [33].

Acknowledgment

The authors would like to thank National Institute of Standards and Technology (NIST) coworkers for technical assistance at Boulder Microfabrication Facility. This paper is a contribution of NIST, an agency of the U.S. government, not subject to U.S. copyright.

References

[1] A. I. Buzdin, "Proximity effects in superconductor-ferromagnet heterostructures," *Rev. Modern Phys.*, vol. 77, pp. 935–976, Jul. 2005.
[2] F. S. Bergeret, A. F. Volkov, and K. B. Efetov, "Long-range proximity effects in superconductor-ferromagnet structures," *Phys. Rev. Lett.*, vol. 86, no. 18, pp. 4096–4099, Apr. 2001.
[3] M. Eschrig, "Spin-polarized supercurrents for spintronics," *Phys. Today*, vol. 64, no. 1, pp. 43–49, Jan. 2011.
[4] M. G. Blamire and J. W. A. Robinson, "The interface between superconductivity and magnetism: Understanding and device prospects," *J. Phys. Condens. Matter*, vol. 26, Oct. 2014, Art. no. 453201.
[5] J. Linder and J. W. A. Robinson, "Superconducting spintronics," *Nature Phys.*, vol. 11, pp. 307–315, Apr. 2015.
[6] V. V. Ryazanov, V. A. Oboznov, A. Y. Rusanov, A. V. Veretennikov, A. A. Golubov, and J. Aarts, "Coupling of two superconductors through a ferromagnet: Evidence for a π junction," *Phys. Rev. Lett.*, vol. 86, pp. 2427–2430, 2001.
[7] T. Kontos, M. Aprili, J. Lesueur, F. Genêt, B. Stephanidis, and R. Boursier, "Josephson junction through a thin ferromagnetic layer: Negative coupling," *Phys. Rev. Lett.*, vol. 89, 2002, Art. no. 137007.
[8] C. Bell, G. Burnell, C. W. Leung, E. J. Tarte, D. J. Kang, and M. G. Blamire, "Controllable Josephson current through a pseudospin-valve structure," *Appl. Phys. Lett.*, vol. 84, no. 7, pp. 1153–1155, Feb. 2004.

[9] M. A. E. Qader, R. K. Singh, S. Galvin, L. Yu, J. M. Rowell, and N. Newman, "Switching at small magnetic fields in Josephson junctions fabricated with ferromagnetic barrier layers," *Appl. Phys. Lett.*, vol. 104, no. 2, Jan. 2014, Art. no. 022602.
[10] B. Baek, W. H. Rippard, S. P. Benz, S. E. Russek, and P. D. Dresselhaus, "Hybrid superconducting-magnetic memory device using competing order parameters," *Nature Commun.*, vol. 5, May 2014, Art. no. 3888.
[11] B. Baek *et al.*, "Spin-transfer torque switching in nanopillar superconducting-magnetic hybrid Josephson junctions," *Phys. Rev. Appl.*, vol. 3, Jan. 2015, Art. no. 011001.
[12] E. C. Gingrich *et al.*, "Controllable 0–π Josephson junctions containing a ferromagnetic spin valve," *Nature Phys.*, vol. 12, pp. 564–567, Mar. 2016.
[13] I. M. Dayton *et al.*, "Experimental demonstration of a Josephson magnetic memory cell with a programmable π-junction," *IEEE Magn. Lett.*, vol. 9, Feb. 2018, Art. no. 3301905.
[14] B. M. Niedzielski, E. C. Gingrich, R. Loloee, W. P. Pratt, and N. O. Birge, "S/F/S Josephson junctions with single-domain ferromagnets for memory applications," *Supercond. Sci. Technol.*, vol. 28, Jul. 2015, Art. no. 085012.
[15] B. Baek, M. L. Schneider, M. R. Pufall, and W. H. Rippard, "Phase offsets in the critical-current oscillations of Josephson junctions based on Ni and Ni-$(Ni_{81}Fe_{19})_xNb_y$ barriers," *Phys. Rev. Appl.*, vol. 7, Jun. 2017, Art. no. 064013.
[16] J. A. Glick *et al.*, "Critical current oscillations of elliptical Josephson junctions with single-domain ferromagnetic layers," *J. Appl. Phys.*, vol. 122, Oct. 2017, Art. no. 133906.
[17] T. Yamashita, A. Kawakami, and H. Terai, "NbN-Based Ferromagnetic 0 and π Josephson Junctions," *Phys. Rev. Appl.*, vol. 8, Nov. 2017, Art. no. 054028.
[18] R. K Singh, N. D. Rizzo, M. Bertram, K. Zheng, and N. Newman, "Improvement in the magnetic properties of Ni-Fe thin films on thick Nb electrodes using oxidation and low energy Ar ion milling," *IEEE Magn. Lett.*, vol. 9, Nov. 2017, Art. no. 5100904.
[19] B. A. Tsukernik, M. Karpovski, and A. Palevski, "Oscillations of the superconducting critical current in Nb-Cu-Ni-Cu-Nb junctions," *Phys. Rev. Lett.* vol. 89, no. 18, Oct. 2002, Art. no. 187004.
[20] V. Shelukhin *et al.*, "Observation of periodic π-phase shifts in ferromagnet-superconductor multilayers," *Phys. Rev. B*, vol. 73, May 2006, Art. no. 174506.
[21] J. W. A. Robinson, S. Piano, G. Burnell, C. Bell, and M. G. Blamire, "Zero to Pi transition in superconductor-ferromagnet-superconductor junctions," *Phys. Rev. B*, vol. 76, Sep. 2007, Art. no. 094522.
[22] A. Bannykh *et al.*, "Josephson tunnel junctions with a strong ferromagnetic interlayer," *Phys. Rev. B*, vol. 79, Feb. 2009, Art. no. 054501.
[23] R. A. Ferrell, "Josephson tunneling and quantum mechanical phase," *Phys. Rev. Lett.*, vol. 15, no. 12, pp. 527–529, Sep. 1965.
[24] A. I. Buzdin, L. N. Bulaevskii, and S. V. Panyukov, "Critical-current oscillations as a function of the exchange field and thickness of the ferromagnetic metal (F) in an S-F-S Josephson junction," *J. Exp. Theor. Phys. Lett.*, vol. 35, no. 4, pp. 178–180, Feb. 1982.
[25] M. Eschrig, "Spin-polarized supercurrents for spintronics: a review of current progress," *Rep. Prog. Phys.*, vol. 78, Sep. 2015, Art. no. 104501.
[26] Z. Radović, N. Lazarides, and N. Flytzanis, "Josephson effect in double-barrier superconductor-ferromagnet junctions," *Phys. Rev. B*, vol. 68, Jul. 2003, Art. no. 014501.
[27] T. Van Duzer and C. W. Turner, *Principles of Superconductive Device and Circuits*, New York, NY, USA: Elsevier, 1981.
[28] E. Goldobin, D. Koelle, R. Kleiner, and A. Buzdin, "Josephson junctions with second harmonic in the current-phase relation: Properties of φ junctions," *Phys. Rev. B*, vol. 76, 2007, Art. no. 224523.
[29] A. Buzdin and A. E. Koshelev, "Periodic alternating 0- and π-junction structures as realization of φ;-Josephson junctions," *Phys. Rev. B*, vol. 67, Jun. 2003, Art. no. 220504(R).
[30] S. M. Frolov, D. J. Van Harlingen, V. V. Bolginov, V. A. Oboznov, and V. V. Ryazanov, "Josephson interferometry and Shapiro step measurements of superconductor-ferromagnet-superconductor 0-π junctions," *Phys. Rev. B*, vol. 74, Jul. 2006, Art. no. 020503(R).
[31] H. Sickinger *et al.*, "Experimental evidence of a φ; Josephson junction," *Phys. Rev. Lett.*, vol. 109, Sep. 2012, Art. no. 107002.
[32] F. S. Bergeret, A. F. Volkov, and K. B. Efetov, "Josephson current in superconductor-ferromagnet structures with a nonhomogeneous magnetization," *Phys. Rev. B*, vol. 64, Sep. 2001, Art. no. 134506.
[33] D. S. Holmes, A. L. Ripple, and M. A. Manheimer, "Energy-efficient superconducting computing—Power budgets and requirements," *IEEE Trans. Appl. Supercond.*, vol. 23, no. 3, Jun. 2013, Art. no. 1701610.

Authors' biographies not available at the time of publication.